The study and analysis of chemical main materials in Li-ion polymer batteries for UAV

Nguyen Van Tu*

Institute of Materials, Biology and Environment, Academy of Military Science and Technology, 17 Hoang Sam, Nghia Do, Hanoi, Vietnam.
*Corresponding author: nguyenvantu882008@gmail.com
Received 19 Aug. 2025; Revised 17 Nov. 2025; Accepted 2 Dec. 2025; Published 25 Dec. 2025.
DOI: https://doi.org/10.54939/1859-1043.j.mst.108.2025.75-82

ABSTRACT

For modern UAVs, the power source is usually a Li-ion polymer battery. Using modern physicochemical analysis methods such as scanning electron microscopy (SEM), energy-dispersive X-ray spectroscopy (EDX), X-ray diffraction (XRD), differential thermogravimetry (TGA), specific surface area (BET) and infrared spectroscopy (FT-IR), we determined the chemical composition of some of the main materials in Li-ion polymer batteries used for drones. We used the method of determining the corresponding size, voltage, and internal resistance to determine some of the main technical indicators of this type of battery. The analysis results show that the Li-ion polymer battery used for UAV has a cubic shape, dimensions of 281×72×5.2 mm (LxWxH), voltage of 3.78 V, internal resistance of 0.456 mΩ, positive electrode material is $LiNi_{0.6}Co_{0.2}Mn_{0.2}O_2$ coated on Al foil, negative electrode material is graphite coated on Cu foil, separator is polyethylene, binder is polyvinylidene fluoride (PVDF), positive electrode side leaf is Al, negative electrode side leaf is Cu. The analysis results also show that both negative and positive electrodes are made of fine, micrometer-sized, uniform powdered materials.

Keywords: Li-polymer; Li-ion; Electrode material; Battery, UAV.

1. INTRODUCTION

Nowadays, unmanned aerial vehicles (UAVs) are widely used in both civil and military [1, 2]. For civil purposes such as: photography, video recording, transportation, delivery, forest management, weather forecasting, agricultural applications, rescue; in military purposes such as: reconnaissance, spying on enemy activities, suicide attacks, security surveillance, information jamming. The energy sources for UAVs are mainly in four forms: Fossil fuels, fuel cells; solar energy and chemical energy (battery). Within the scope of the study, the article only focuses on the type of UAVs that use chemical energy sources, using electric motors to operate [3-5]. The chemical energy source for this type of UAV requires high specific capacity, light weight, stable voltage and discharge current, designed to withstand thermal shock, small and compact. And the power source based on Li-ion or Ni-MH meets these technical requirements [6].

A Li-ion battery is a rechargeable battery in which lithium ions move from the negative electrode to the positive electrode during discharge and move back to the negative electrode when the battery is charged. A typical Li-ion battery consists of a positive electrode, a negative electrode, a separator, and an electrolyte. The positive electrode is made of transition metal oxide compounds such as: $LiMnO_2$, $LiCoO_2$, $LiMn_2O_4$, $LiFePO_4$, $LiNiO_2$ or their spinel form $LiNi_{1-x-y}Co_xMn_yO_2$, combined with conductive carbon powder, binder and coated on aluminum foil [7-9]. The negative electrode is usually made of graphite coated on a thick copper foil that stores the Li+ ions in the crystal [10-12]. A thin porous separator made of polyethylene or polypropylene, 15 µm to 25µm thick, is placed between the positive and negative electrodes [10, 13]. The electrolyte is usually a Li^+-containing salt such as $LiPF_6$, $LiClO_4$, $LiBF_4$, dissolved in an organic solvent, such as ethylene carbonate, dimethyl carbonate, and diethyl carbonate, or a mixture of them, and a flame retardant additive [6, 10].

Classifying Li-ion batteries by electrolyte, Li-ion batteries have 3 main types: Liquid electrolyte (Li-ion), gel or polymer electrolyte (Li-ion polymer, or abbreviated LiPo) and solid electrolyte (Li-ion solid electrolyte, abbreviated (SSBs- Lithium solid-state batteries). Compared with liquid electrolytes and solid organic electrolytes, polymer electrolytes have advantages such as better resistance to volume changes of the electrode during charging and discharging, improved safety, good flexibility and processability. These batteries provide higher specific energy than other lithium-ion batteries. Therefore, LiPo batteries are mainly used for remote control (RC) devices, such as remote control cars, drones/UAVs, remote control aircraft/helicopters, and flying and photography devices (FPV - First Person View) that connect and transmit to the control device on the ground [2, 14, 15]. The operating principle of LiPo batteries is shown in figure 1 [16].

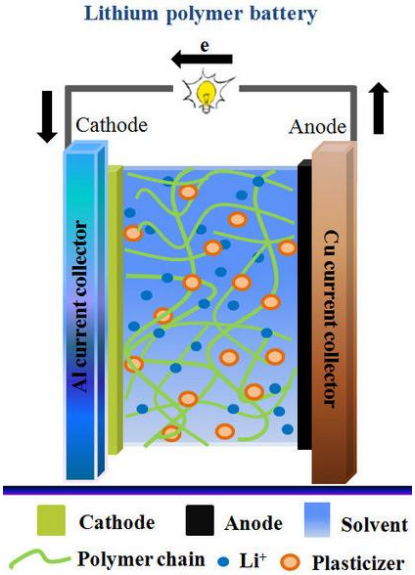

Figure 1. *The principle of the LiPo battery [16].*

The reaction occurs at the electrodes (cathode, anode) and the overall reaction is shown in the equations below:

Positive electrode (cathode):

$$LiMO_2 \underset{Discharge}{\overset{Charge}{\rightleftarrows}} Li_{1-x}MO_2 + xLi^+ + xe \quad (1)$$

M is the transition metals of group VIII, such as Ni, Co, Mn.

Negative electrode (anode):

$$C + xLi^+ + xe \underset{Discharge}{\overset{Charge}{\rightleftarrows}} Li_xC \quad (2)$$

Total reaction:

$$LiMO_2 + C \underset{Discharge}{\overset{Charge}{\rightleftarrows}} Li_xC + Li_{1-x}MO_2 \quad (3)$$

To contribute to the research and orientation of LiPo battery testing technology, in this paper, we present the results of chemical composition analysis of the negative electrode, positive electrode and separator of the battery for UAV, after use.

2. EXPERIMENT AND METHODS

2.1. Experimental method

The prismatic polymer Li-ion battery sample has dimensions of 281×72×5.2 mm (length ×

width × height), a weight of 295 g, determining the electrochemical parameters, showing: voltage 3.78 V, internal resistance 0.456 mΩ. Then discharge the battery to 2.0V, and proceed with the steps to disassemble the battery. Voltage and internal resistance measurements are performed with an electric meter (Japan), with an error of 1mV and an error of 0.01mΩ. The sample LiPo battery was manually disassembled by cutting the outer shell with a mechanical cutter to separate the positive electrode, negative electrode and separator layer. After disassembly, the materials were separated, washed with solvent and electrolyte several times in alcohol solution. Then, they were washed 3 times with distilled water, dried at 80 ºC for 12 hours, stored and analyzed. The thickness of the positive electrode, negative electrode and separator foil was measured to be 30 µm, 25 µm and 25 µm, respectively. For the positive electrode material sample analyzed by ICP-MS method, prepare as follows: weigh 0.1 g of material, put it in 10 ml of concentrated HNO_3, heat it and add boiling ice, after diluting to 1 liter, proceed with analysis.

2.2. Research methods

The main material in LiPo batteries were analyzed by physicochemical analysis such as SEM-EDX analysis using S4800-Hitachi (Japan), differential thermal analysis (TGA) on Netzsch TGA209F1 (with P-type detector; TG-sample aluminum), crystal structure analysis by X-ray diffraction method on Bruker D5005 (Germany), Fourier transform infrared spectroscopy (FT-IR) on Nexus 670/Nicolet (USA) and surface area analysis (BET) on TriStar II 3020 (Version 3.02). Determination of trace Li+ion concentrations using inductively coupled plasma mass spectrometry (ICP-MS) (ICAPRQ02904, Thermofisher Scientific).

3. RESULT AND DISCUSSION

3.1. Chemical composition analysis of positive electrode material

The positive electrode is a plate-shaped electrode consisting of active material coated on the electrode foil. To determine the elemental composition of the positive electrode active material, energy dispersive spectroscopy (SEM-EDX), XRD analysis methods are used and the analysis results are shown in figure 2.

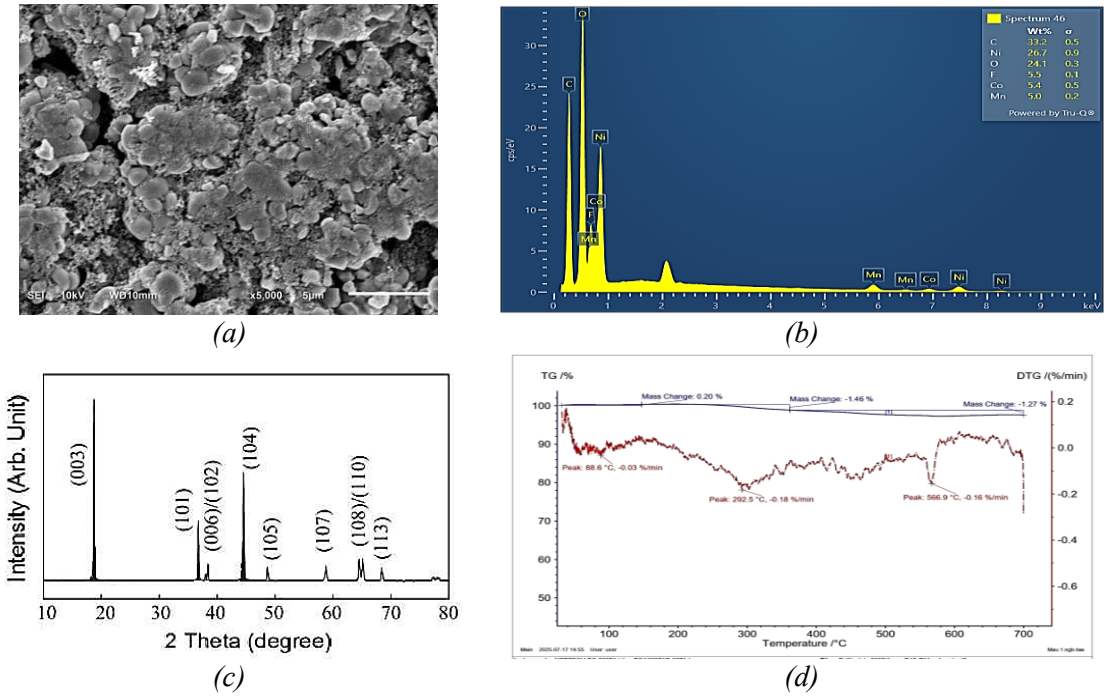

Figure 2. *Analysis of the positive electrode: (a) SEM image; (b) EDX; (c) XRD; (d) TGA .*

From the SEM image analysis results in figure 2(a), it can be seen that the positive electrode material has a surface, uniformly distributed particles and a particle size of 1 μm. The XRD and EDX analysis results show that the spinel structure of $LiMO_2$, M consists of Ni, Co and Mn metals, mixed with conductive carbon. The result is $LiNi_{1-x-y}Co_xMn_yO_2$, with Ni as the majority element, and Co and Mn as additives to improve the mechanical and physical properties of the $LiNiO_2$ material. In the EDX analysis results, the elements C and F are found in the electrode material containing conductive graphite powder, and F may be contained in the binder (polyvinylidene fluoride (PVDF)). The element Li does not appear in the EDX spectrum due to the limitations of the equipment, which cannot detect light elements such as Li. To confirm the presence of Lithium (Li) element in the active material of the positive electrode, we analyzed the material sample by inductively coupled plasma mass spectrometry (ICP-MS). The analysis results showed that the concentration of Li^+ ions in the positive electrode material was about 98 mg/L.

According to the authors [17], $LiNi_xCo_yMn_zO_2$ (NCM) layered material has a high specific capacity and a lower price than $LiCoO_2$ material, often used as a positive electrode material to replace $LiCoO_2$. In this group of materials, there are NCM variants such as: NCM111 ($LiNi_{1/3}Co_{1/3}Mn_{1/3}O_2$); NCM523 ($LiNi_{0.5}Co_{0.2}Mn_{0.3}O_2$); NCM622 ($LiNi_{0.6}Co_{0.2}Mn_{0.2}O_2$); NCM811 ($LiNi_{0.8}Co_{0.1}Mn_{0.1}O_2$). From the EDX analysis results, we can calculate the molar ratio of Ni, Co, Mn in the corresponding compound as: 26.7/58: 5.4/59:5.0/55= 0.4564:0.0915:0.0909, by rounding this ratio to the sum of 1, we get the corresponding ratio as: 0.5743: 0.2084:0.2163, rounding we get the ratio Ni:Co:Mn as 0.6:0.2:0.2. Comparing these calculation results and the NCM forms, it can be deduced that the spinel compound used as the positive electrode material is $LiNi_{0.6}Co_{0.2}Mn_{0.2}O_2$. Comparing the EDX analysis results and NCM forms, it can be inferred that the spinel compound used as a positive electrode material is $LiNi_{0.6}Co_{0.2}Mn_{0.2}O_2$. XRD analysis results show the characteristic peaks of the hexagonal structure group (R3m) of the NCM material group, at the characteristic peaks 19.3°, 38.5°, 44.8°, 58.5° corresponding to the reflection planes (003), (101), (104), (107). Thermal analysis shows that the positive electrode active substance is thermally stable above 600 ºC. At temperatures of 88.6 ºC, the evaporation of the adsorbed electrolyte component on the electrode occurs (0.2% mass loss), at 292.5 ºC, the decomposition of the PVDF binder occurs (1.46% mass loss), at 567 ºC, the complete decomposition of the PVDF binder occurs (1.27% mass loss). This result is consistent with the analysis results of PVDF binder published previously by Dr. Carolin Fischer [18].

3.2. Chemical composition analysis of negative electrode material

From the SEM image analysis results in figure 3(a), it can be seen that the negative electrode material sample has a smooth surface, uniformly distributed particles, and a particle size of 5 μm. The EDX and XRD analysis results show that the active material component of the negative electrode is mainly carbon (97.5%) and has a structure typical of graphite material. The XRD analysis results (figure 3(c)) show that the carbon form in the active material of the negative electrode has a crystal structure equivalent to graphite crystal at the characteristic peaks 26.4°, 42.3°, 44.5°, 54.5° corresponding to the reflection planes (002), (100), (101), (004). In which, the peak at position 26.4° is formed with a sharp peak, narrow foot, high band intensity, corresponding to the distance between 2 adjacent layers d(002) = 0.333 nm, characteristic of the graphite crystal form of carbon.

Thermal analysis shows that the positive electrode active material is thermally stable above 600 ºC, in this temperature range, it almost does not decompose or lose mass. The results of the specific surface area analysis (BET) show that the material has a large specific surface area of 4.541 m^2/g. The above analysis results indicate that the negative electrode material of the sample battery has graphite as the main component, similar to commercial Li-ion polymer batteries [6, 9].

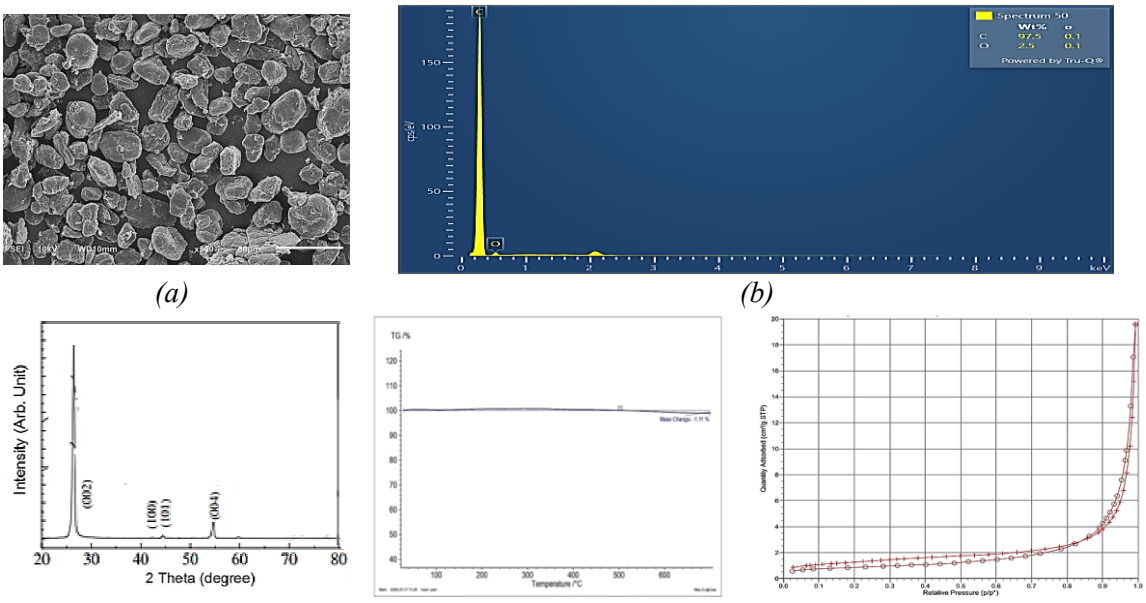

(a) *(b)* *(c)* *(d)* *(e)*

Figure 3. *Analysis of negative electrode: (a) SEM image; (b) EDX; (c) XRD; (d) TGA; (f) BET.*

3.3. Chemical composition analysis of separator materials

From the SEM image analysis results in figure 4(a), it can be seen that the leaf material sample has a porous surface, evenly distributed, with a pore size of about 0.1 µm. The infrared analysis results (FT-IR) show the characteristics of the polyethylene functional group, compared with the standard sample, with the following wavelengths: 2920, 2848 corresponding to the C-H bond in the CH_2 group, 1462 corresponding to the C-H bond in the CH_3 group, and 730 corresponding to the C=C group. Thermal analysis shows that the insulation material is heat-resistant. At 477.1 ^oC, the material decomposes, losing 91% of its mass, corresponding to the decomposition process of polyethylene. From the results of FT-IR analysis, thermal analysis, and SEM image analysis, it is shown that the insulation material is polyethylene, with a porous structure [13].

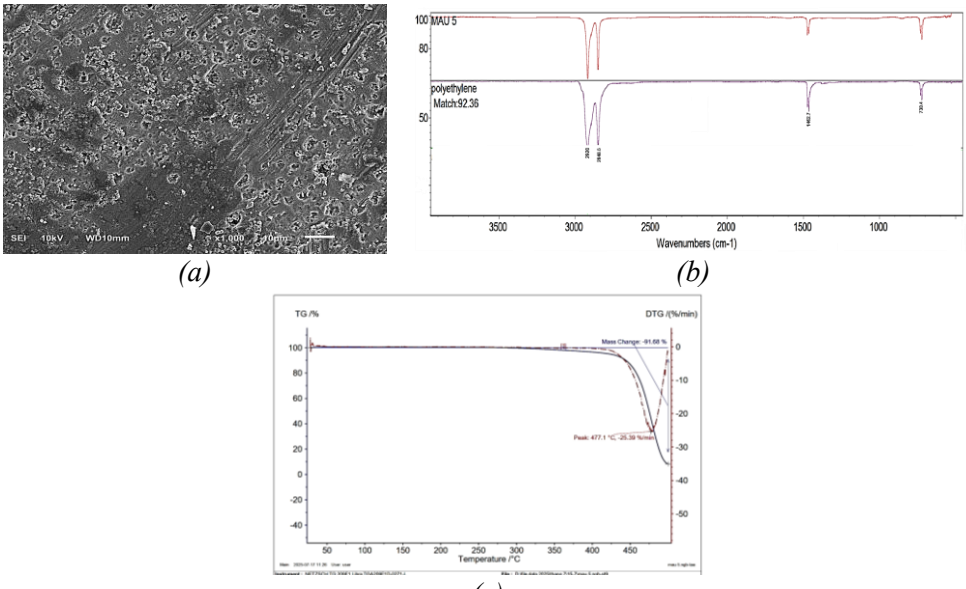

(a) *(b)*

(c)

Figure 4. *Analysis of the separator: (a) SEM image; (b) FT-IR; (c) TGA.*

3.4. Chemical composition analysis of positive electrode foil

From the SEM image analysis results in figure 5(a), it can be seen that the positive electrode foil material has a smooth, even surface. The EDX and XRD analysis results show the characteristics of the aluminum (Al) element. The EDX analysis only contains Al (93.9%) and the remaining O (6.1%), proving that the sample contains aluminum, without any other elements, and the O content in the EDX analysis results is due to the fact that the aluminum foil surface contains an ultra-thin layer of aluminum oxide (Al_2O_3) [12]. The XRD diagram (figure 5(c)) shows the peaks at 2θ values of 38.4°; 44.7°; 65.1° and 78.5°, which are equivalent to the peaks of the standard spectrum of cubic aluminum crystals, space group Fm3m corresponding to the (111), (200), (220) and (311) planes, respectively.

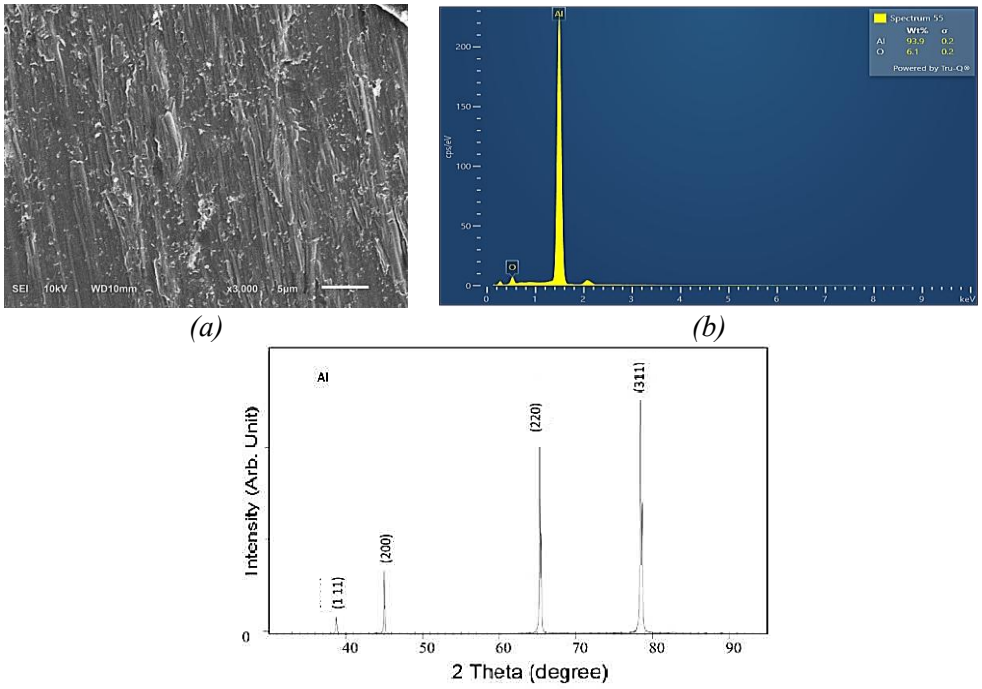

***Figure 5**. Analysis of the positive electrode foil: (a) SEM image; (b) EDX; (c) XRD.*

3.5. Chemical composition analysis of negative electrode foil

From the SEM image analysis results in figure 6(a), it can be seen that the negative electrode rib material sample has a smooth, flat surface. The EDX and XRD analysis results show the characteristics of pure copper (Cu) element. The EDX analysis only contains copper (98.0%) and also contains O (2.0%), proving that the sample contains copper, without any other elements, and the O content in the EDX analysis results is due to the presence of an ultra-thin layer of copper oxide (such as Cu_2O, CuO) on the surface of the copper foil [11]. Based on the XRD results in figure 6(c), it can be seen that the XRD diffraction peaks of the cathode flank at 2θ values of 43°, 50° and 74° coincide with the characteristic peaks of cubic uniform crystals, space group Fm3m corresponding to the (111), (200) and (220) faces.

4. CONCLUSIONS

The LiPo battery sample was disassembled and analyzed for the main components of the materials used for the negative electrode, positive electrode, electrode plate and separator. The analysis results show that the main active material of the cathode is $LiNi_{0.6}Co_{0.2}Mn_{0.2}O_2$ (NCM622) and has added conductive carbon additives, PVDF binder mixed uniformly, then coated on

aluminum foil with a thickness of about 30 μm. The negative electrode is mainly composed of graphite and binder additives mixed homogeneously and coated on a 25 μm-thick copper foil. The material used as the insulator is polyethylene, porous, with a pore size of about 0.1 μm. The analysis results are the basis for designing and manufacturing a battery with dimensions and electrochemical parameters equivalent to the sample battery.

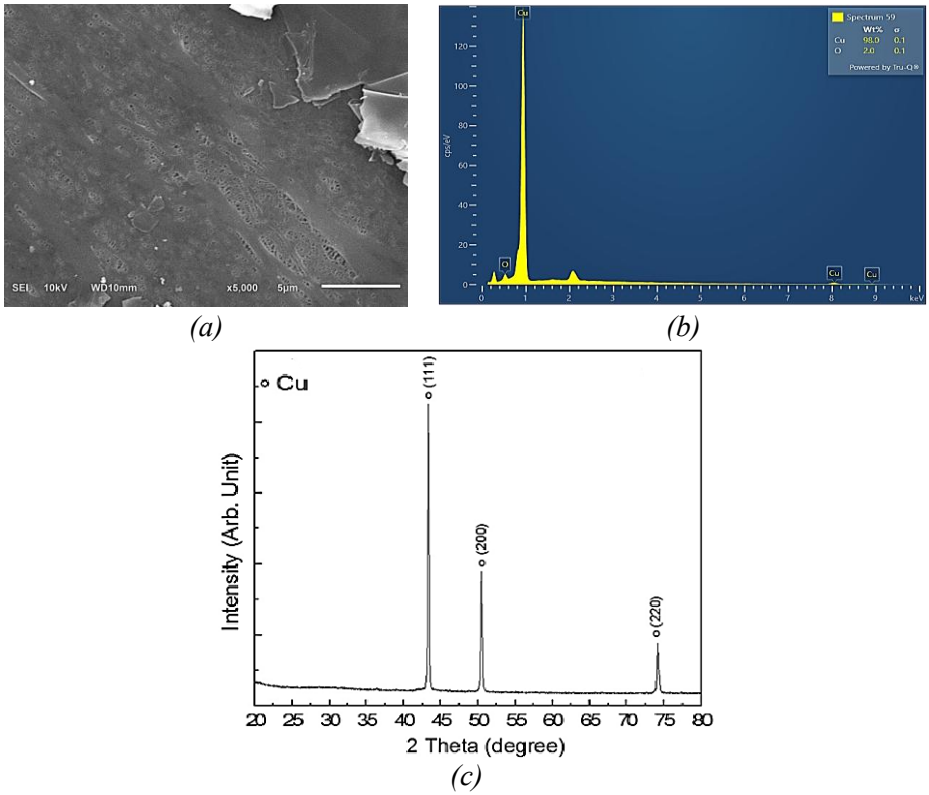

Figure 6. *Analysis of the negative electrode foil: (a) SEM image; (b) EDX; (c) XRD.*

REFERENCE

[1]. Asif A. Laghari, Awais K. Jumani, Rashid A. Laghari, and Haque Nawaz, *"Unmanned aerial vehicles: A Review"*, Cognitive Robotics, Vol. 3, pp. 8–22, (2023).

[2]. Fan Bangkui, Li Yun, Zhang Ruiyu, and Fu Qiqi, *"Review on the Technological Development and Application of UAV Systems"*, Chinese Journal of Electronics, Vol. 29, No. 2, pp. 119–207, (2020).

[3]. Chun Xiao, Bin Wang, Dan Zhao, Chao Wang, *"Comprehensive investigation on lithium batteries for electric and hybrid-electric unmanned aerial vehicle applications"*, Thermal Science and Engineering Progress, Vol. 38, Article 101677, (2023).

[4]. Y. Zhang, Z. Li, Y. Huang, B. Cui, J. Zhou, and Y. Guo, *"Modelling and simulation of high- and low-speed impact damage of lithium batteries for light and small UAVs"*, International Journal of Impact Engineering, Vol. 180, Article 104703, (2023).

[5]. F. Nex, C. Armenakis, M. Cramer, D. A. Cucci, M. Gerke, E. Honkavaara, A. Kukko, C. Persello, and J. Skaloud, *"UAV in the advent of the twenties: Where we stand and what is next"*, ISPRS Journal of Photogrammetry and Remote Sensing, Vol. 184, pp. 215–242, (2022).

[6]. N. Nitta, F. Wu, J. T. Lee, and G. Yushin, *"Li-ion battery materials: present and future"*, Materials Today, Vol. 18, No. 5, pp. 252–264, (2015).

[7]. X. Zhou, Y. Zhou, L. Yu, S. Hu, and S. Y. Lee, *"Gel polymer electrolytes for rechargeable batteries toward wide-temperature applications"*, Chemical Society Reviews, Vol. 53, pp. 5291–5325, (2024).

[8]. H. Li, L. Wang, L. Wang, Y. Song, Z. Zhang, H. Zhang, A. Du, and X. He, *"Significance of current collectors for high performance conventional lithium-ion batteries: A review"*, Advanced Functional Materials, Vol. 33, No. 49, Article 2305515, (2023).

[9]. Alex K. Koech, Gershom Mwandila, Francis Mulolani, and Phenny Mwaanga, *"Lithium-ion battery fundamentals and exploration of cathode materials: A review"*, South African Journal of Chemical Engineering, Vol. 50, No. 5, pp. 321–339, (2024).
[10]. Navid N. Esfahani, Hamid Garmestani, Mohsen Bagheritabar, Dheyaa J. Jasim, D. Toghraie, and Hooman Firoozeh, *"Comprehensive review of lithium-ion battery materials and development challenges"*, Renewable and Sustainable Energy Reviews, Vol. 203, Article 114783, (2024).
[11]. Lei Yang, Wei Weng, Huanlin Zhu, Xiaopeng Chi, Wen Tan, Zhen Wang, and Shuiping Zhong, *"Preparing ultra-thin copper foil as current collector for improving the LIBs performances with reduced carbon footprint"*, Materials Today Communications, Vol. 35, Article 105952, (2023).
[12]. Mustafa Khan, Suxia Yan, Mujahid Ali, Faisal Mahmood, and Yong Wang, *"Innovative solutions for high-performance silicon anodes in lithium-ion batteries: Overcoming challenges and real-world applications"*, Nano-Micro Letters, Vol. 16, Article 179, (2024).
[13]. Dafaalla M. D. Babiker, Zubaida R. Usha, Caixia Wan, Mohmmed M. Elseed Hassaan, Xin Chen, and Liang B. Li, *"Recent progress of composite polyethylene separators for lithium/sodium batteries"*, Journal of Power Sources, Vol. 564, Article 232853, (2023).
[14]. Abdul G. Olabi, Qaisar Abbas, Pragati A. Shinde, Mohammad A. Abdelkareem, *"Rechargeable batteries: Technological advancement, challenges, current and emerging applications"*, Energy, Vol. 266, No. 1, Article 126408, (2023).
[15]. Ghassan Zubi et al., *"The Li-ion battery: State of the art and future perspectives"*, Renewable and Sustainable Energy Reviews, Vol. 89, pp. 292–308, (2018).
[16]. *"Lithium polymer battery"*, Wikipedia, https://en.wikipedia.org/wiki/Lithium_polymer_battery.
[17]. Chen L., Bang Tong, Shi Li, Ze S. Wei, Jin H. Sun, and Qing S. Wang, *"Role of transition metal ratio on electrochemical and thermal properties of LiNixCoyMnzO2 layered materials for lithium-ion batteries"*, Transactions of Nonferrous Metals Society of China, Vol. 34, pp. 1936–1950, (2024).
[18]. Carolin Fischer, *"Characterization of PVDF binder for Li-ion batteries by means of TGA-FT-IR"*, NETZSCH-Gerätebau GmbH, Selb, Germany, (2019).

TÓM TẮT

Nghiên cứu, phân tích thành phần hóa học các vật liệu chính của pin Li-ion polymer trong bộ nguồn UAV

Với các UAV hiện đại, nguồn điện sử dụng thường là pin Li-ion polymer. Sử dụng các phương pháp phân tích hóa lý hiện đại như kính hiển vi điện tử quét (SEM), phổ tán xạ năng lượng tia X (EDX), phổ nhiễu xạ tia X (XRD), nhiệt vi sai (TGA), diện tích bề mặt riêng (BET) và phổ hồng ngoại (FT-IR) chúng tôi đã xác định được thành phần hóa học của một số vật liệu chính trong pin Li-ion polymer dùng cho UAV. Đồng thời sử dụng phương pháp xác định kích thước, điện áp, nội trở tương ứng để xác định một số chỉ tiêu kỹ thuật chính của loại pin này. Kết quả phân tích cho thấy, pin Li-ion polymer dùng cho UAV có dạng hình lập phương, kích thước 281×72×5,2 mm (DxRxC), điện áp 3,78 V, điện trở nội 0,456 mΩ, vật liệu điện cực dương là LiNi0.6Co0.2Mn0.2O2 phủ trên lá Al, vật liệu điện cực âm là graphite phủ trên lá Cu, màng ngăn cách là polyethylene, chất kết dính là polyvinylidene fluoride (PVDF), lá sườn điện cực dương là Al, lá sườn điện cực âm là Cu. Kết quả phân tích cũng cho thấy cả điện cực âm và điện cực dương đều được làm từ vật liệu dạng bột, mịn, kích thước micromet, đồng đều.

Từ khóa: Li-polymer; Li-ion; Vật liệu điện cực; Pin, UAV.